



## Modern human atlas ranges of motion and Neanderthal estimations

Carlos A. Palancar<sup>a,\*</sup>, Markus Bastir<sup>a</sup>, Antonio Rosas<sup>a</sup>, Pierre-Michel Dugailly<sup>b</sup>, Stefan Schlager<sup>c</sup>, Benoit Beyer<sup>d</sup>

<sup>a</sup> Group of Paleoanthropology, Department of Paleobiology, Museo Nacional de Ciencias Naturales (CSIC), Madrid, Spain

<sup>b</sup> Department of Diagnostic and Therapeutic Technologies CESPU – Escola Superior de Saúde Do Vale Do Ave, Famalicao, Portugal

<sup>c</sup> Biological Anthropology, University Medical Center, Freiburg, Germany

<sup>d</sup> Université Libre de Bruxelles, Laboratory for Functional Anatomy, Brussels, Belgium

### ARTICLE INFO

#### Keywords:

Cervical vertebra

Mobility

Hominin

Flexion–extension

Rotation

## 1. Introduction

### 1.1. Biomechanics of the cervical vertebrae

Classically, it has been hypothesized that there is a relationship between cervical spine kinematics and vertebrae morphology in both modern humans (Nowitzke et al., 1994; Cattrysse et al., 2011; Hallgren et al., 2011; Siccardi et al., 2020) and non-human primates (Demes, 1985; Strait and Ross, 1999; Bogduk and Mercer, 2000; Mercer and Bogduk, 2001; Gommery, 2006). Indeed, more recent works tried to demonstrate the existence of a relationship between vertebral morphology and locomotor behavior and neck posture within the order Primates (Manfreda et al., 2006; Parks, 2012; Grider-Potter and Hallgren, 2013; Nalley, 2013; Nalley and Grider-Potter, 2015, 2017; Meyer et al., 2018). However, the possible relationship between neck ranges of motion (ROM) and cervical vertebrae morphology has not been directly studied until recently (Cattrysse et al., 2011; Grider-Potter et al., 2020). In their pioneering study Grider-Potter et al. (2020) tested the general hypothesis that the bony morphology of cervical vertebrae had an influence on neck ranges of motion in a sample of 12 species of primates with different locomotor patterns, including *Homo sapiens*. They performed up to 43 regression analyses (between ROM and different linear measurements), obtaining only three statistically significant outputs. Given this low significance ratio, Grider-Potter et al. (2020) concluded that the bony morphology of cervical vertebrae probably did not play a

primary role in determining neck ROM. However, other studies focused on *H. sapiens* such as Nowitzke et al. (1994) found that some cervical spine morphological features are partially related with kinematics (i.e., the height of the zygapophyseal joints influences the axes of rotation). This is in line with more research in modern humans (Clausen et al., 1997; Penning and Wilmink, 1987; Cattrysse et al., 2011) and the ‘relaxation model’, that allows less head and neck stiffness in bipedal hominins—compared to African great apes—as the head becomes balanced above the vertical line of gravity (Schultz, 1942; Meyer and Haeusler, 2015; Meyer et al., 2017).

Even so, none of the previous works have studied the three-dimensional (3D) bony shape, focusing their analyses in a few traditional measurements. In this context, here we try to improve the methodology previously used, studying the possible relationship between modern human atlas morphology and upper cervical spine mobility, testing the null hypothesis ( $H_0$ ) of no relationship between them.

### 1.2. The Neanderthal cervical column

Although the neck and cervical vertebrae of Neanderthals have not been studied in depth until very recently, several works conclude that Neanderthal neck would be less lordotic and more stable than that of modern humans (Gómez-Olivencia et al., 2013; Been et al., 2017; Been and Bailey, 2019). However, the mobility of the Neanderthal cervical

\* Corresponding author.

E-mail address: [palancar.carlos@gmail.com](mailto:palancar.carlos@gmail.com) (C.A. Palancar).

<https://doi.org/10.1016/j.jhevol.2023.103482>

Received 28 February 2023; Received in revised form 11 December 2023; Accepted 11 December 2023

Available online 18 December 2023

0047-2484/© 2023 The Authors. Published by Elsevier Ltd. This is an open access article under the CC BY-NC-ND license (<http://creativecommons.org/licenses/by-nc-nd/4.0/>).

spine has not been studied up to now. Palancar et al. (2020b) showed differences of the modern human and Neanderthal atlas morphology at the level of the superior articular facets (SAFs): they were flatter on Neanderthals. Thus, assuming the presumptions of Mercer and Bogduk (2001) that more concave articular facets allow a greater mobility, atlanto-occipital ROM would be lower in *Homo neanderthalensis*, which matches previous works hypotheses (Gómez-Olivencia et al., 2013; Been and Bailey, 2019; Been et al., 2017). Even so, these are only assumptions as no functional analyses have been made on Neanderthal atlases. Thus, a more exhaustive analysis is necessary to check whether inferences made so far, based only on some morphological characters, are true or not. To this end, we estimate ROM of seven fossil individuals belonging to the species *H. neanderthalensis*.

## 2. Material and methods

### 2.1. Material

The modern human sample consists of eight unembalmed bodies analyzed in previous works (Dugailly et al., 2010), where dissections consisted of removing the superficial soft tissues to access the upper cervical spine and its connected anatomical structures such as ligaments, suboccipital muscles and fascia. All these structures were kept intact, while the lower cervical segment (below the third cervical vertebra), mandible and anterior viscera of the neck were removed. More about specimen preparation can be found elsewhere (Dugailly et al., 2010, 2011, 2013). The fossil sample consists of seven Neanderthal atlases. Two atlases come from Krapina site, in Croatia (Kr.98 and Kr.100; Radović et al., 1988; Palancar et al., 2020a). Two atlases are from El Sidrón site, in Spain (SD-1643 and SD-1605; Rosas et al., 2006; Palancar et al., 2020b). The atlases of La Chapelle-aux-Saints 1 (Boule, 1911-1913; Gómez-Olivencia, 2013) and La Ferrassie 1 (Heim, 1976; Gómez-Olivencia et al., 2018), from France, and that of Kebara 2, from Israel (Arensburg, 1991) were also included.

### 2.2. Kinematic data

Ranges of motion in both flexion–extension and rotation were obtained from previous work (Dugailly et al., 2010; Beyer et al., 2020). Each anatomical preparation was set on a custom-made jig and fixed on a rigid plate. Kinematics were analyzed from five sagittal positions in two different motions: 1) flexion–extension, from neutral to intermediate and maximal flexion and extension; 2) rotation, from neutral to intermediate and maximal right and left rotation. On each discrete position, spatial locations of the bones were recorded using a 3D-digitalizer (FARO, B06/Rev 18). The output of discrete joint displacements was analyzed according to a standard mathematical method for processing motion computation in order to obtain ROM in degrees (Capozzo et al., 1995). Details about the whole experimental set-up and validation protocol can be found elsewhere (Dugailly et al., 2010, 2011, 2013; Beyer et al., 2020).

### 2.3. Shape analysis

In order to analyze the morphological variation of the unembalmed atlas, imaging acquisition were performed on each specimen using computed tomography (Siemens SOMATOM, helical mode, reconstruction: slice thickness = 0.5 mm, inter-slice spacing = 1 mm, image data format = DICOM) by Dugailly et al. (2011). Segmentation and 3D model reconstruction were performed using semi-automatic procedures on the software Amira v 3.0. (Van Sint Jan et al., 2002). For the first time, these 3D models were studied following standard protocols of 3D geometric morphometrics (Bastir et al., 2019). Starting from an original template described by Palancar et al. (2021), several subsets, described in Supplementary Online Material (SOM) Table S1 and SOM Fig. S1, were analyzed in order to find the regions of atlas more related to mobility.

- Full morphology: all landmarks and semilandmarks covering the entire shape. We measure the full shape, including the morphology of the arches and its structures (i.e. the groove for the cervical artery).
- Without the arches: semilandmarks of the anterior and posterior arches are removed. This way we reduce the number of variables—as the number of variables influence on the results is under discussion (Cardini, 2020)—but we still measure the attachment point of ligaments and muscles in transverse processes and both anterior and posterior tubercles, as well as the fovea dentis.
- Lateral masses: landmarks and semilandmarks of the anterior and posterior arches and transverse processes are removed. This subset reduces the focus to the shape of both superior and inferior articular facets, but still including information about the height of the vertebra.
- Both superior articular facets: only landmarks and semilandmarks of the SAFs. This way we analyze the atlanto-occipital joint exclusively.
- One superior articular facet: only landmark and semilandmarks of the left SAF. Focusing on one facet alone, we can test whether the facet tropism (Brailsford, 1929) affects to ROM or not.
- Both inferior articular facets (IAFs): only landmarks and semilandmarks of the IAFs. This way we analyze the atlanto-axial joint exclusively.

### 2.4. Morpho-functionality analysis

In order to check that independent variables follow a normal distribution, we performed Shapiro-Wilk analyses (Shapiro and Wilk, 1965). In addition, to check if there is an allometric relationship in the sample and, therefore, analyses should be corrected for the effect of size, a prior regression is performed between the shape of each of the landmark subsets and the centroid size of the individuals (Klingenberg, 2016). Then, to test the possible relation between the atlas shape and ROM, we performed partial least squares (PLS) analyses, as they are more reliable than regression analyses when the number of variables (landmarks) exceed the number of observations (Geladi and Kowalski, 1986; Farahani et al., 2010). Given that the number of PLS analyses performed on each subset is high (12), we applied Bonferroni adjustments on each to assess multiple-testing artefacts (Bland and Altman, 1995).

### 2.5. Neanderthals range of motion estimations

Using the function ‘predictPLSfromData’ of ‘Morpho’ v. 1.5.1 package (Schlager, 2017) run in RStudio v. 4.3.0 (Posit team, 2023), and on the basis of the PLS-type analyses performed previously, we can obtain the estimated ROM of a new individual, from the coordinates of the landmarks covering the morphology of the fossil. In order to validate this model for estimating unknown ranges of motion, a leave-one-out cross-validation was performed on each significant PLS (Stone, 1974). Then, quadratic mean error of predicted values of the cross-validations were calculated. Finally, to check if there are significant differences between Neanderthals and modern humans, we performed Student’s t-tests in RStudio.

## 3. Results

### 3.1. Morpho-functional analysis

Motion data are summarized in SOM Table S2. All these variables presented non-significant values in the Shapiro-Wilk test, so that their normality is accepted and, therefore, they can be analyzed by PLS. The regressions performed between the shape variable and centroid size for each of the landmark subsets show non-significant results, indicating that there is no clear allometric relationship and the PLS should not be corrected for size. Out of a total of 72 PLS, eight show a high significance

( $p < 0.05$ ; Table 1). After Bonferroni adjustments, only the two PLS with a  $p < 0.01$  remained significant. Of all the subsets, the lateral masses and one SAF showed the greatest statistical significance and correlation with ROM. In contrast, IAFs did not show statistical significance in any of the PLS performed. Between the different movements studied, it is the rotation which presents the greatest number of significant analyses in relation to shape. Figures 1 and 2 show that atlas morphologies associated with lower mobility maintain a common pattern in all regressions and motion types: SAFs are concave, elongated and narrow. On the other hand, atlases associated with higher mobility have flatter, shorter and wider SAFs. In addition, Figure 1 shows that less mobile atlases have greater projection of the anterior and posterior tubercles, a greater vertebral height and a lower anteroposterior diameter.

### 3.2. Neanderthal atlases estimations

Supplementary Online Material Table S3 shows both the estimates for the fossil individuals and the values of the modern human sample for comparison, along with the group means. The estimated values for the Neanderthal individuals are very similar to those presented by modern humans. In fact, in the mean comparison analyses performed between these two groups for each of the subsets and movements, it is concluded that there are no significant differences in any of them (SOM Table S4). To help in the interpretation of the data, Figure 3 shows motion values (estimated for Neanderthals and real for modern humans) in a box-and-violin diagram, where it can be observed that the ROM of Neanderthal individuals falls within the modern human range of variation in every motion. It is noteworthy that the estimates are congruent among the different subsets and movements, since, with some exceptions, El Sidrón individuals present high mobility values, while Kebara 2 Neanderthal presents the lowest (SOM Table S3). Regarding the error of ROM estimates, it varies between 1 and 8° depending on the motion and the subset. For example, in rotation, between C0 and C2, the real mean ROM is 55.31 (SOM Table S2) and the margin of error is 7° (Table 1).

## 4. Discussion

This is the first study in which the 3D bony shape of the modern human atlas is analyzed under a kinematics approach, assessing its possible relation with ROM. Taking into account the proportion of statistically significant PLS regressions presented here (11% and even lower after Bonferroni adjustment), atlas shape influence on ranges of motion is doubtful. Even so, there is a great congruence of the results obtained in the visualization of shapes associated with the different ROM. All statistically significant PLS show coincident results: greater atlas mobility is related to flatter and shorter SAFs (Figs. 1 and 2). This finding, although tentative, could change our understanding on the mobility of the upper neck and its joints. While previous works (Bogduk and Mercer, 2000; Mercer and Bogduk, 2001; Aiello and Dean, 2002) hypothesized that the greater length of the articular facets or their greater convexity would increase joint mobility, none of these have directly tested the morpho-functional relationship of the cervical vertebrae nor, in particular, the atlas. Contrary to what was previously hypothesized and in view of these preliminary results shown here, shorter and flatter SAFs could increase the mobility of the upper neck region.

Regarding the flatness, the explanation may be related to the bony constraint exerted by the anterior and posterior walls of atlas SAF. As explained by Bogduk and Mercer (2000), the atlanto-occipital joint would find the limit of flexion–extension range in the anterior and posterior walls of the SAFs, which end up ‘colliding’ with the occipital condyles. When these articular facets are flat, the anterior and posterior walls would barely exert a limit, causing the ROM of this joint to increase. Our finding matches the conclusion of Hallgren et al. (2011), who found that younger individuals had flatter SAFs than older ones and hypothesized that this could be the reason why infants or children are

**Table 1** Partial least squares (PLS) analyses performed on the kinematic data of the specimens and the morphology of their atlas, collected by different subsets of landmarks. Error is measured in degrees.<sup>a</sup>

Variables	Full shape			Without arches			Lateral masses			Both SAFs			One SAF			Both IAFs			
	Error	p	Correlation coefficient	Error	p	Correlation coefficient	Error	p	Correlation coefficient	Error	p	Correlation coefficient	Error	p	Correlation coefficient	Error	p	Correlation coefficient	
Extension																			
C0-C1	-	0.541	85.82	-	0.617	90.81	-	0.578	87.35	-	0.418	75.81	-	0.189	75.95	-	0.433	72.43	-
C1-C2	-	0.734	84.88	-	0.73	80.98	-	0.811	72.71	-	0.861	82.14	-	0.844	76.07	-	0.653	76.91	-
C0-C2	4.27	0.037	89.94*	-	0.514	91.23	-	0.543	89.53	-	0.452	87.89	-	0.572	75.94	-	0.301	73	-
Flexion																			
C0-C1	-	0.372	96.95	-	0.221	98.25	-	0.147	92.65	2.18	0.049	86.5*	1.68	0.003	95.46**	-	0.652	71.24	-
C1-C2	-	0.923	92.09	-	0.875	78.25	-	0.747	76.83	-	0.39	69.5	-	0.501	80.38	-	0.938	85.83	-
C0-C2	-	0.471	94.65	-	0.448	91.67	-	0.368	87.26	-	0.178	77.09	-	0.127	75.72	-	0.534	70.53	-
Flexion–extension																			
C0-C1	-	0.242	93.92	-	0.253	96.73	-	0.23	92.94	-	0.069	88	2.79	0.012*	94.85*	-	0.818	73.82	-
C1-C2	-	0.213	90.5	-	0.135	91.11	-	0.201	85.09	-	0.379	79.64	-	0.488	65.17	-	0.666	83.37	-
C0-C2	-	0.071	93.18	2.85	0.025	98.08*	-	0.139	94.02	-	0.144	91.81	-	0.124	77.86	-	0.897	72.09	-
Rotation																			
C0-C1	-	0.218	97.61	2.34	0.045	98.48*	1.75	0.007	98.82**	-	0.096	90.45	-	0.158	79.42	-	0.606	79.88	-
C1-C2	-	0.398	96.02	-	0.193	94.93	-	0.098	95.83	-	0.058	87.3	-	0.171	76.51	-	0.494	72.17	-
C0-C2	-	0.36	96.63	-	0.066	96.55	7.07	0.029*	98.09*	-	0.056	89.71	-	0.158	78.18	-	0.515	73.92	-

Abbreviations: p = p-value; SAF = superior articular facet; IAF = inferior articular facet; C0 = occipital; C1 = atlas; C2 = axis.  
<sup>a</sup> Significance levels are indicated by asterisks. A single or double asterisk means high significance (\* =  $p < 0.05$ ; \*\* =  $p < 0.01$ ). Underlined coefficients are those that remained significant after Bonferroni adjustments.

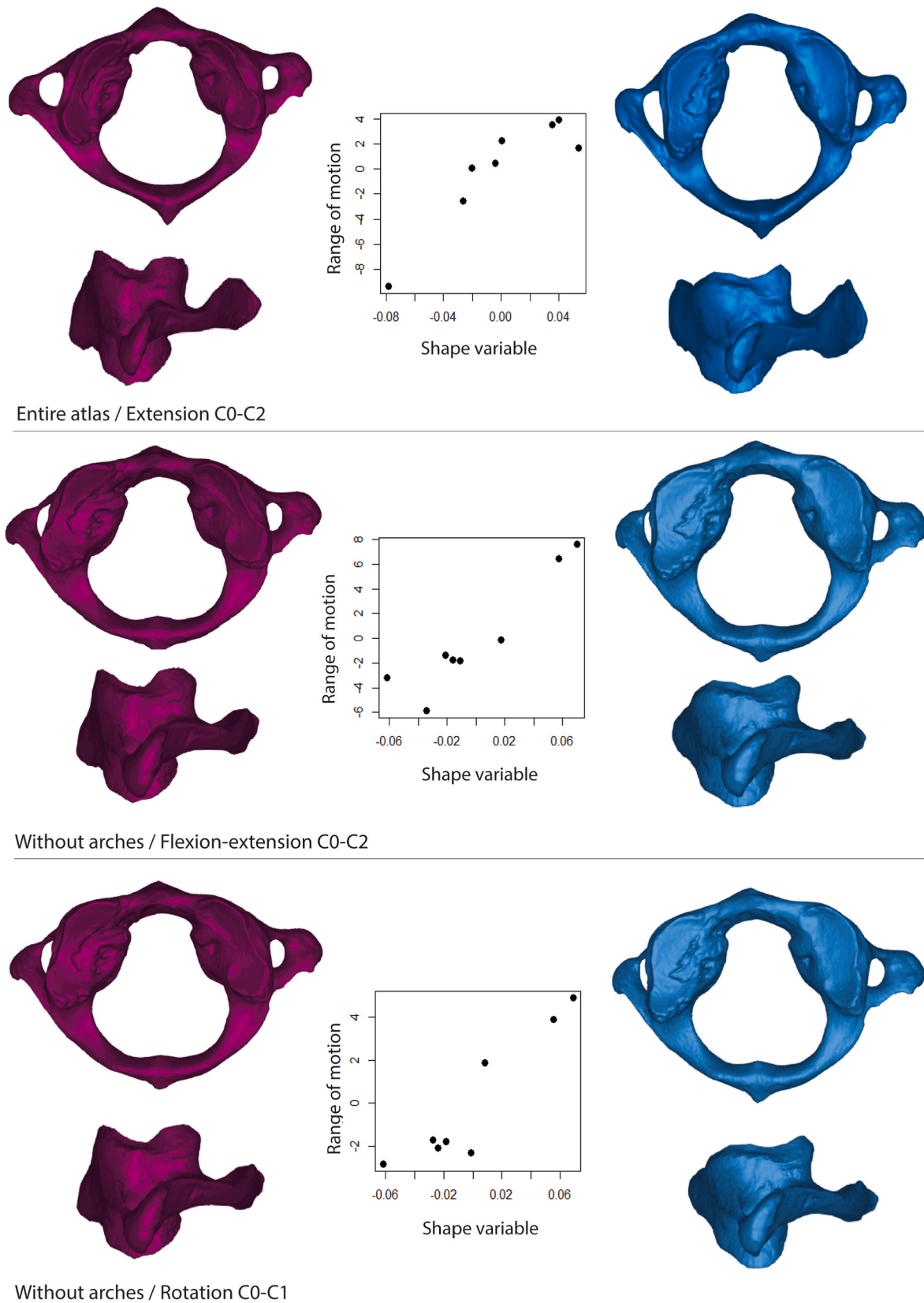


**Fig. 1.** Partial least squares (PLS) performed on the entire atlas morphology and without arches subsets and visualizations of the associated morphologies. On the left, morphologies associated with lower mobility. On the right, morphologies associated with higher mobility. Each model is presented in superior view (top) and right lateral view (bottom). Abbreviations: C0 = occipital; C1 = atlas; C2 = axis.

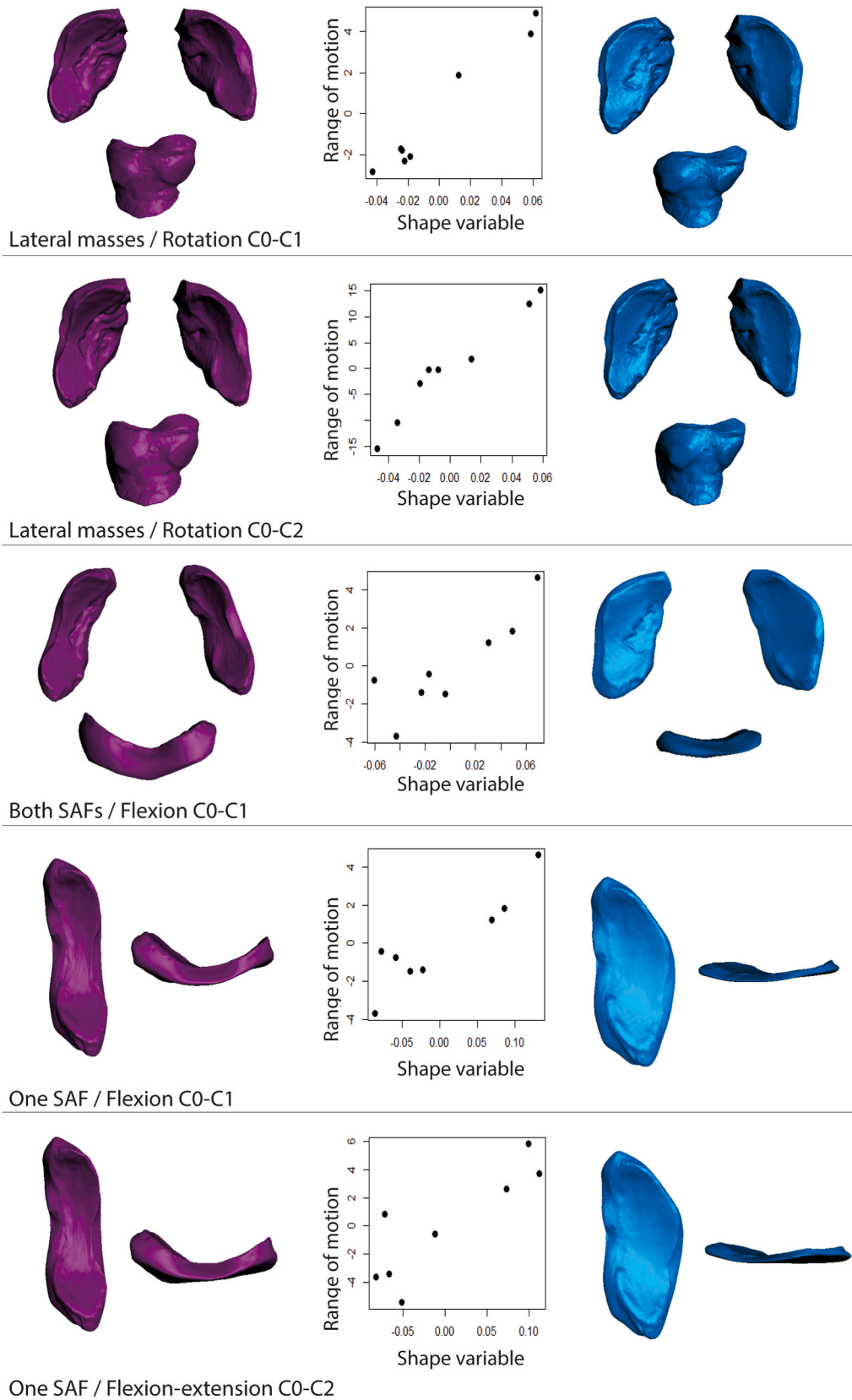


**Fig. 2.** Partial least squares (PLS) performed on different subsets (lateral masses, both superior articular facets [SAFs], and one superior articular) and visualizations of the associated morphologies. On the left, morphologies associated with lower mobility. On the right, morphologies associated with greater mobility. Each model is presented in superior view (top) and right lateral view (bottom). Abbreviations: C0 = occipital; C1 = atlas; C2 = axis.

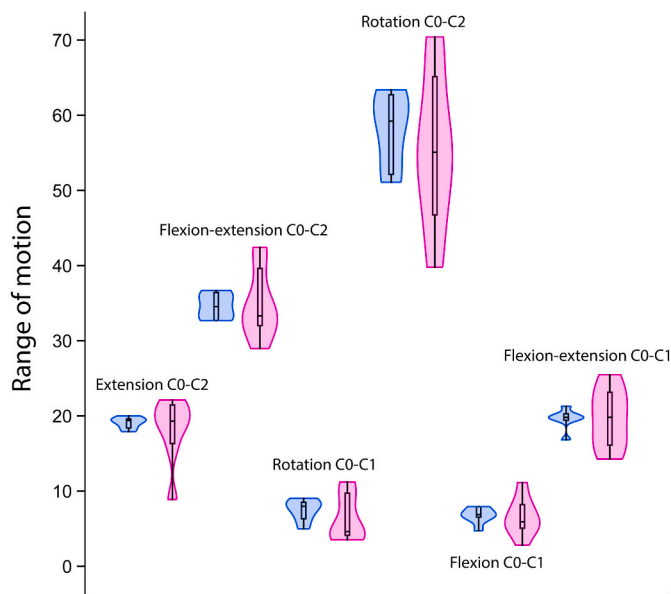


**Fig. 3.** Box and jitter plot of the estimated Neanderthal ranges of motion (left, blue) and real distribution of modern humans (right, pink) in statistically significant motions. When the same motion is significant in different subsets, the most correlated partial least square is shown. Abbreviations: C0 = occipital; C1 = atlas; C2 = axis. (For interpretation of the references to colour in this figure legend, the reader is referred to the Web version of this article.)

more vulnerable to whiplash injuries of the neck.

The fact that the shorter length of SAFs is associated with greater mobility is more difficult to explain. Although different from a functional perspective, the carpal joint is morphologically similar to the atlanto-occipital. Hamrick (1996) showed that length of the articular surfaces of the carpals does not differ between locomotor groups of Primates. Even so, the relation between the length of an articular facet functionally similar to the SAF of atlas and its mobility is, to our knowledge, unknown and requires future and more exhaustive analyses.

It is important to note that none of the ROM measured between C1 and C2 is related to shape. All statistically significant PLS involve ROM between C0 and C1 ( $n = 3$ ) or C0 and C2 ( $n = 5$ ). This fact, together with the lack of statistically significant PLS on the subsets of the IAFs, could indicate that the atlanto-axial joint shape is not related to mobility. This is logical since the atlanto-axial joint at the level of the lateral facets is conditioned by the convex cartilage that covers them (Mercer and Bogduk, 2001). In fact, this joint undergoes what is known as paradoxical atlanto-axial motion during neck flexion–extension and also a passive, counter-axial motion during lateral tilt (Mercer and Bogduk, 2001). In both movements, the atlanto-axial joint demonstrates a somewhat ‘random’ behavior that can have little influence on ROM, as demonstrated here.

#### 4.1. Fossil atlases

In light of the preliminary results presented here, our concept of the biomechanics of the Neanderthal cervical spine needs to be examined and discussed in depth. The Neanderthal neck has so far been understood as more stable in the sagittal, coronal and transverse planes due to the proportions of the cervical vertebrae and the projection and orientation of their tubercles and processes, as well as the cranial base morphology (Gómez-Olivencia et al., 2013). However, although these results are tentative and the studied region should be extended to the entire cervical spine, the present experimental and innovative data suggest that the Neanderthal neck may not be more stable than that of modern humans, but of similar biomechanical characteristics to them.

Although the concavity of SAFs of Neanderthal atlases appears to be

slightly lower than in modern humans (Palancar et al., 2020a), these differences seem insufficient to cause differences in the ROM of the upper cervical spine, as shown by mean comparison analyses (SOM Table S4). Moreover, not only the morphology of SAFs influences ROM, but also their relative orientation. This is similar in modern humans and Neanderthals, and could be related to the similarity of the estimated motion values found for Neanderthals compared to *H. sapiens*.

The present results performed on the bone morphology of the Neanderthal atlas do not support the hypothesis that there were differences between their mobility of the upper cervical spine and that of modern humans. However, the interacting function of the ligaments and musculature is yet to be determined and will be the subject of future research in order to improve and deepen our understanding of the morpho-functionality of the neck as a whole.

#### 4.2. Study limitations

In conducting this research on cervical spine motion in modern human cadaveric samples and extrapolating the findings to predict the potential mobility in Neanderthals, several limitations must be acknowledged. Firstly, the study is challenged by the inherent anatomical differences between modern humans and Neanderthals. For example, the greater anteroposterior dimension of the occipital base in Neanderthals (Bastir et al., 2011) would slightly modify the spatial relation and orientation of muscles and ligaments attached to atlas and axis and thus, exert a different moment arm and limitation to mobility. Secondly, the PLS predictions are susceptible to a margin of error spanning from one to seven degrees, potentially impacting the accuracy of these predictions. Nonetheless, research conducted on cadaveric samples to assess ranges of motion in modern humans have similarly demonstrated an error range of approximately two degrees (Van Sint Jan et al., 2002; Martelli, 2003; Dugailly et al., 2011). As a result, the error in our predictions regarding the range of motion in Neanderthals is comparable to the error observed in the data acquisition for modern humans. Lastly, it is essential to recognize the inherent disparity between studying cadaveric specimens and living individuals, as the latter’s dynamic physiological factors, such as muscle tone and neurological control, can significantly influence the actual range of motion experienced by a living hominin. Despite these limitations, this investigation provides valuable insights into understanding the potential cervical mobility in Neanderthals and serves as a foundation for further research in this area. Future studies should increase the region of study and the sample, as the ROM varies between sexes, populations and groups of age (Pan et al., 2018).

#### CRedit authorship contribution statement

**Carlos A. Palancar:** Conceptualization, Formal analysis, Investigation, Validation, Writing - original draft. **Markus Bastir:** Conceptualization, Funding acquisition, Investigation, Supervision, Writing - review & editing. **Antonio Rosas:** Data curation, Funding acquisition, Writing - review & editing. **Pierre-Michel Dugailly:** Data curation, Formal analysis. **Stefan Schlager:** Methodology, Software. **Benoit Beyer:** Conceptualization, Investigation, Methodology, Supervision, Writing - review & editing.

#### Acknowledgments

The Spanish Ministry of Science and Innovation funds this research via two national projects (PID 2020-115854 GB-I00 and PID 2021-122356NB-I00) and one technician grant (PTA 2020-018205-I). We acknowledge Martin Friess (Musée de l’Homme, Paris), Davorka Radovčić (Croatian Natural History Museum, Zagreb), Ofer-Bar-Yosef (Harvard University), Bernard Vandermeersch (Université de Bordeaux), Baruch Arensburg and Israel Hershkovitz (Tel Aviv University) for providing permissions to study the fossil specimens. Finally, we

acknowledge the co-Editor-in-Chief (Clément Zanolli), the Associate Editor, and three anonymous reviewers for their careful comments improving an earlier version of this study.

## Supplementary Online Material

Supplementary Online Material to this article can be found online at <https://doi.org/10.1016/j.jhevol.2023.103482>.

## References

- Aiello, L., Dean, C., 2002. Human Evolutionary Anatomy: An Introduction to Human Evolution. Academic Press, London.
- Arensburg, B., 1991. The vertebral column, thoracic cage and hyoid bone. In: Bar-Yosef, O., Vandermeersch, B. (Eds.), *Le Squelette Moustérien de Kebara 2*. Editions du CNRS, Paris, pp. 113–147.
- Bastir, M., García-Martínez, D., Torres-Tamayo, N., Palancar, C.A., Fernández-Pérez, F.J., Riesco-López, A., Osborne-Márquez, P., Ávila, M., López-Gallo, P., 2019. Workflows in a virtual morphology lab: 3D scanning, measuring, and printing. *J. Anthropol. Sci.* 97, 1–28.
- Bastir, M., Rosas, A., Gunz, P., Peña-Melian, A., Manzi, G., Harvati, K., Kruszynski, R., Stringer, C., Hublin, J.-J., 2011. Evolution of the base of the brain in highly encephalized human species. *Nat. Commun.* 2, 588.
- Been, E., Bailey, J., 2019. The association between spinal posture and spinal biomechanics in modern humans: Implications for extinct hominins. In: Been, E., Gómez-Olivencia, A., Krammer, P.A. (Eds.), *Spinal Evolution*. Springer, Cham, pp. 283–299.
- Been, E., Shefi, S., Soudack, M., 2017. Cervical lordosis: The effect of age and gender. *Spine J.* 17, 880–888.
- Beyer, B., Feipel, V., Dugailly, P.M., 2020. Biomechanics of the upper cervical spine ligaments in axial rotation and flexion-extension: Considerations into the clinical framework. *J. Craniovertebr Junction Spine* 11, 217–225.
- Bland, J.M., Altman, D.G., 1995. Multiple significance tests: The Bonferroni method. *Br. Med. J.* 310, 170.
- Bogduk, N., Mercer, S., 2000. Biomechanics of the cervical spine. I: Normal kinematics. *Clin. Biomech.* 15, 633–648.
- Boule, M., 1911–1913. L'Homme fossile de La Chapelle-aux-Saints. *Ann. Paleontol.* 6, 111–172, 7, 21–56, 85–192; 8, 1–70.
- Brailsford, J.F., 1929. Deformities of the lumbosacral region of the spine. *Br. J. Surg.* 16, 562–627.
- Cappozzo, A., Catani, F., Della Croce, U., Leardini, A., 1995. Position and orientation in space of bones during movement: Anatomical frame definition and determination. *Clin. Biomech.* 10, 171–178.
- Cardini, A., 2020. Less tautology, more biology? A comment on “high-density” morphometrics. *Zoomorphology* 139, 513–529.
- Catrysse, E., Probyn, S., Kool, P., Clarys, J.P., Van Roy, P., 2011. Morphology and kinematics of the atlanto-axial joints and their interaction during manual cervical rotation mobilization. *Man. Ther.* 16, 481–486.
- Clausen, J.D., Goel, V.K., Traynelis, V.C., Scifert, J., 1997. Uncinate processes and Luschka joints influence the biomechanics of the cervical spine: Quantification using a finite element model of the C5–C6 segment. *J. Orthop. Res.* 15, 342–347.
- Demes, B., 1985. Biomechanics of the Primate Skull Base. Springer-Verlag, Berlin.
- Dugailly, P.M., Sobczak, S., Sholukha, V., Van Sint Jan, S., Salvia, P., Feipel, V., Rooze, M., 2010. In vitro 3D-kinematics of the upper cervical spine: Helical axis and simulation for axial rotation and flexion extension. *Surg. Radiol. Anat.* 32, 141–151.
- Dugailly, P.M., Sobczak, S., Moiseev, F., Sholukha, V., Salvia, P., Feipel, V., Rooze, M., Van Sint Jan, S., 2011. Musculoskeletal modeling of the suboccipital spine: Kinematics analysis, muscle lengths, and muscle moment arms during axial rotation and flexion extension. *Spine* 36, E413–E422.
- Dugailly, P.M., Sobczak, S., Lubansu, A., Rooze, M., Van Sint Jan, S., Feipel, V., 2013. Validation protocol for assessing the upper cervical spine kinematics and helical axis: An in vivo preliminary analysis for axial rotation, modeling, and motion representation. *J. Craniovertebr. Junction Spine* 4, 10.
- Farahani, H.A., Rahiminezhad, A., Same, L., Immanezhad, K., 2010. A comparison of partial least squares (PLS) and ordinary least squares (OLS) regressions in predicting of couples mental health based on their communicational patterns. *Procedia Soc. Behav. Sci.* 5, 1459–1463.
- Geladi, P., Kowalski, B.R., 1986. Partial least-squares regression: A tutorial. *Anal. Chim. Acta* 185, 1–17.
- Gómez-Olivencia, A., Been, E., Arsuaga, J.L., Stock, J.T., 2013. The Neandertal vertebral column I: The cervical spine. *J. Hum. Evol.* 64, 608–630.
- Gommery, D., 2006. Evolution of the vertebral column in Miocene hominoids and Pliocene hominids. In: Ishida, H., Tuttle, R., Pickford, M., Ogiwara, N., Nakatsukasa, M. (Eds.), *Human Origins and Environmental Backgrounds*. Springer, New York, pp. 31–43.
- Grider-Potter, N., Hallgren, R.C., 2013. Atlantooccipital joint orientation and posture in catarrhines. *Am. J. Phys. Anthropol.* 150, 137, 137.
- Grider-Potter, N., Nalley, T.K., Thompson, N.E., Goto, R., Nakano, Y., 2020. Influences of passive intervertebral range of motion on cervical vertebral form. *Am. J. Phys. Anthropol.* 172, 300–313.
- Gómez-Olivencia, A., 2013. Back to the old man's back: Reassessment of the anatomical determination of the vertebrae of the Neandertal individual of La Chapelle-aux-Saints. *Ann. Paleontol.* 99, 43–65.
- Gómez-Olivencia, A., Quam, R., Sala, N., Bardey, M., Ohman, J.C., Balzeau, A., 2018. La Ferrassie 1: New perspectives on a “classic” Neandertal. *J. Hum. Evol.* 117, 13–32.
- Hallgren, R.C., Catrysse, E., Zrull, J.M., 2011. In vitro characterization of the anterior to posterior curvature of the superior articular facets of the atlas as a function of age. *Spine J.* 11, 241–244.
- Hamrick, M.W., 1996. Articular size and curvature as determinants of carpal joint mobility and stability in strepsirrhine primates. *J. Morphol.* 230, 113–127.
- Heim, J.L., 1976. *Les Hommes Fossiles de La Ferrassie I: Le Gisement, les Squelettes Adultes (Crâne et Squelette du Tronc)*. Masson, Paris.
- Klingenberg, C.P., 2016. Size, shape, and form: Concepts of allometry in geometric morphometrics. *Dev. Gene. Evol.* 226, 113–137.
- Manfreda, E., Mitteroecker, P., Bookstein, F.L., Schaefer, K., 2006. Functional morphology of the first cervical vertebra in humans and nonhuman primates. *Anat. Rec.* 289, 184–194.
- Martelli, S., 2003. New method for simultaneous anatomical and functional studies of articular joints and its application to the human knee. *Comput. Methods Progr. Biomed.* 70, 223–240.
- Mercer, S.R., Bogduk, N., 2001. Joints of the cervical vertebral column. *J. Orthop. Sports Phys. Ther.* 31, 174–182.
- Meyer, M.R., Haeussler, M., 2015. Spinal cord evolution in early *Homo*. *J. Hum. Evol.* 88, 43–53.
- Meyer, M.R., Williams, S.A., Schmid, P., Churchill, S.E., Berger, L.R., 2017. The cervical spine of *Australopithecus sediba*. *J. Hum. Evol.* 104, 32–49.
- Meyer, M.R., Woodward, C., Tims, A., Bastir, M., 2018. Neck function in early hominins and suspensory primates: Insights from the uncinate process. *Am. J. Phys. Anthropol.* 166, 613–637.
- Nalley, T.K., Grider-Potter, N., 2015. Functional morphology of the primate head and neck. *Am. J. Phys. Anthropol.* 156, 531–542.
- Nalley, T.K., Grider-Potter, N., 2017. Functional analyses of the primate upper cervical vertebral column. *J. Hum. Evol.* 107, 19–35.
- Nalley, T.K., 2013. Positional behaviors and the neck: A comparative analysis of the cervical vertebrae of living primates and fossil hominoids. Ph.D. Dissertation, Arizona State University.
- Nowitzke, A., Westaway, M., Bogduk, N., 1994. Cervical zygapophyseal joints: Geometrical parameters and relationship to cervical kinematics. *Clin. Biomech.* 9, 342–348.
- Palancar, C.A., Torres-Tamayo, N., García-Martínez, D., García-Tabernero, A., Rosas, A., Bastir, M., 2020a. Comparative anatomy and 3D geometric morphometrics of the El Sidrón atlases (C1). *J. Hum. Evol.* 149, 102897.
- Palancar, C.A., García-Martínez, D., Radović, D., Llidó, S., Mata-Escolano, F., Bastir, M., Sanchis-Gimeno, J.A., 2020b. Krapina atlases suggest a high prevalence of anatomical variations in the first cervical vertebra of Neanderthals. *J. Anat.* 237, 579–586.
- Palancar, C.A., García-Martínez, D., Cáceres-Monllor, D., Perea-Pérez, B., Ferreira, M.T., Bastir, M., 2021. Geometric Morphometrics of the human cervical vertebrae: Sexual and population variations. *J. Anthropol. Sci.* 99, 97–116.
- Pan, F., Arshad, R., Zander, T., Reitmaier, S., Schroll, A., Schmidt, H., 2018. The effect of age and sex on the cervical range of motion—A systematic review and meta-analysis. *J. Biomech.* 75, 13–27.
- Parks, H., 2012. Functional morphology of the atlas in primates and its implications for reconstructing posture in fossil taxa. M.Sc. Thesis, Western Illinois University.
- Penning, L., Wilimink, J.T., 1987. Rotation of the cervical spine: A CT study in normal subjects. *Spine* 12, 732–738.
- Posit team, 2023. RStudio. Integrated development environment for R. Posit Software, PBC, Boston. <https://www.posit.co/>.
- Radović, J., Smith, F.H., Trinkaus, E., Wolpoff, M.H., 1988. The Krapina Hominids: an Illustrated Catalog of the Skeletal Collection. Mladost and the Croatian Natural History Museum, Zagreb.
- Rosas, A., Martínez-Maza, C., Bastir, M., García-Tabernero, A., Lalueza-Fox, C., Huguet, R., Ortiz, J.E., Julià, R., Soler, V., Torres, T., Martínez, E., Cañaveras, J.C., Sánchez-Moral, S., Cuezva, S., Lario, J., Santamaría, D., de la Rasilla, M., Fordea, J., 2006. Paleobiology and comparative morphology of a late Neandertal sample from El Sidrón, Asturias, Spain. *Proc. Natl. Acad. Sci. USA* 103, 19266–19271.
- Schlager, S., 2017. Morpho and Rvcg - shape Analysis in R: R-packages for geometric morphometrics, shape analysis and surface manipulations. In: Zheng, G., Li, S., Szekeley, G. (Eds.), *Statistical Shape and Deformation Analysis*. Academic Press, London, pp. 217–256.
- Schultz, A.H., 1942. Conditions for balancing the head in primates. *Am. J. Phys. Anthropol.* 29, 483–497.
- Shapiro, S.S., Wilk, M.B., 1965. An analysis of variance test for normality (complete samples). *Biometrika* 52, 591–611.
- Siccardi, D., Buzzatti, L., Marini, M., Catrysse, E., 2020. Analysis of three-dimensional facet joint displacement during two passive upper cervical mobilizations. *Musculoskelet. Sci. Pract.* 50, 102218.
- Stone, M., 1974. Cross-validatory choice and assessment of statistical predictions. *J. R. Stat. Soc. B* 36, 111–133.
- Strait, D.S., Ross, C.F., 1999. Kinematic data on primate head and neck posture: Implications for the evolution of basicranial flexion and an evaluation of registration planes used in paleoanthropology. *Am. J. Phys. Anthropol.* 108, 205–222.
- Van Sint Jan, S., Salvia, P., Hilal, I., Sholukha, V., Rooze, M., Clapworthy, G., 2002. Registration of 6-DOFs electrogoniometry and CT medical imaging for 3D joint modeling. *J. Biomech.* 35, 1475–1484.